MATHEMATICAL MODELING OF COMPOSITE FILTER FOR POWER QUALITY IMPROVEMENT OF ELECTRIC ARC FURNACE DISTRIBUTION NETWORK

deepak C. BHONSLE, Electrical Engineering Department, Maharaja Sayajirao University of Baroda, Vadodara, INDIA, dcbhonsle@gmail.com

ramesh B. KELKAR, Electrical Engineering Department, Maharaja Sayajirao University of Baroda, Vadodara, INDIA

Abstract: *This paper presents mathematical modeling of composite filter (CF) for power quality improvement of electric arc furnace (EAF) distribution network. The composite filter is consisting of a shunt passive filter (SHPF) connected with a lower rated voltage source pulse width modulation (PWM) converter based series active power filter (SAPF). A state-space averaging model of a CF is constructed to analyze its system stability by traditional control strategy taking into account the effect of the time delay. The control strategy adopted for composite filter operation is based on simultaneous detection of source current and load voltage harmonic based on the vectorial theory dual formulation of instantaneous reactive power. Simulation for a typical EAF distribution network with a composite power filter has been carried out to validate the performance. Simulation results are shown in an attempt to verify the mathematical model of the filter. The simulations have been carried out in MATLAB environment using SIMULINK and power system block set toolboxes.*

Index Terms— Active filter, harmonics, harmonic distortion, arc, mathematical modeling, stability analysis

1. Introduction

The increasing popularity of EAF in metallurgical industries to melt scrap causes significant impacts on power system and on electrical power quality. EAF is one of responsible source for deteriorating the power quality in the connected network. An EAF is chosen as an industrial non-linear load to demonstrate power quality problems.

Harmonic distortion in power distribution systems can be suppressed using two approaches namely, passive and active powering. The passive filtering is the simplest conventional solution to mitigate the harmonic distortion [1]. Although simple, the use passive elements do not always respond correctly to the dynamics of the power distribution systems. Although simple and least expensive, the passive filter inherits several shortcomings [2]. Combined operation of SAPF with traditional SHPF i.e. composite filter (CF) is found one of the solutions to overcome the disadvantages of the existing passive filters. It controlled to act as a harmonic isolator between the source and nonlinear load by injection of a controlled harmonic voltage source [3-5]. A control algorithm for a three-phase series APF is proposed as shown in Fig. 1.

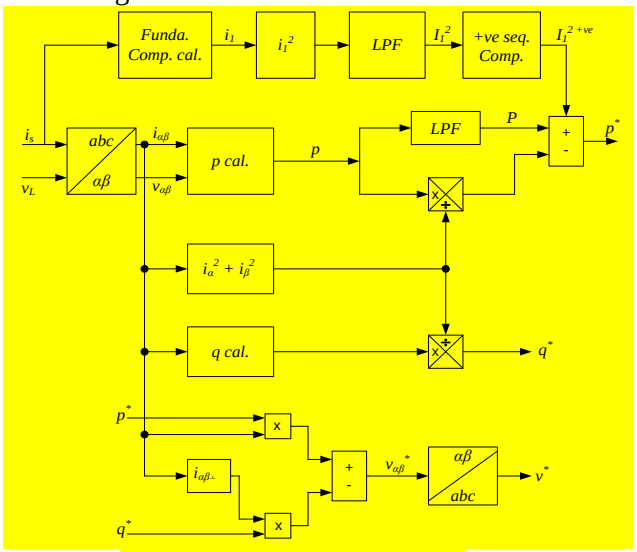

Fig. 1 Control algorithm for CF

The control strategy is based on the vectorial theory dual formulation of instantaneous reactive

power [5], so that the voltage waveform injected by the active filter is able to compensate the reactive power and the load current harmonics and to balance asymmetrical loads. Here an attempt is made to apply the same theory for unbalanced and non-sinusoidal voltage conditions for randomly varying load as an electric arc furnace (EAF).

System stability during CF operation is also one of the important factors from control aspects. Choice of a suitable gain to ensure a good compensation is a tedious and difficult task while keeping the system stable for different load and source condition [6-8]. The analysis and experimental results have pointed out that a time delay can cause a stability problem [9-11, 13]. Hence, a state-space averaging model of composite filter is constructed to analyze the stability problem by traditional control strategy taking into account the delay time. Bode plot of open-loop transfer function concludes that larger time delay could results into phase angle loss seriously leading to system unstable and poor filter performance. A new leading compensating control strategy discussed in [12-14] is applied for enhancing the system stability, for improving the filter performance and for reducing the power rating of the active part. The simulations have been carried out in MATLAB environment using SIMULINK and power system block set toolboxes to validate the same. The paper is organized as follows: Second section deals with the mathematical modeling of EAF as non-linear load. Third section discusses the stability analysis. Fourth section shows various calculations involved in stability analysis. Fifth section deals with the analysis of simulation results. Sixth section concludes the paper.

2. EAF Modeling as Non-linear Load

A. *Main circuit configuration*

The system configuration of a CF consists of a SAPF with a SHPF is shown in Fig. 2.

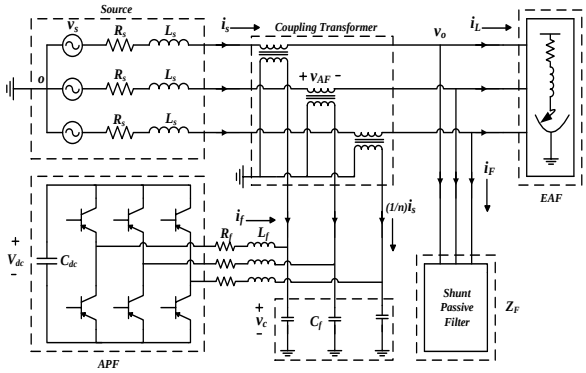

Fig. 2 Main system configuration

Main circuit configuration can be divided into four parts: (a) an ac main (b) SAPF (c) SHPF (d) EAF as non-linear load. SAPF can also be further sub-divided into three parts: (a) a three phase bridge Inverter (generating harmonic voltage for compensation) (b) a Second order Carrier-wave filter (applied to filter the switching frequency component) (c) a Coupling transformer (connected between the electric network and the load with transformation ratio= n).

B. *System Modeling*

The output of voltage of the inverter v_c changes between $\pm V_{dc}$ when the IGBTs are switching. The inverter output voltage is represented by:

$$v_c = V_{dc} \cdot (2 \cdot V - 1) \tag{1}$$

Where, $V = [0,1]$, represents the input discrete values of IGBTs. The controlled output voltage v_c so generated will constrain the harmonics produced by the load. The state-Space averaged mod v el in the stationary frame of reference is described as follows:

Applying KCL at node we get:

$$C_f \cdot \frac{dv_c}{dt} = \frac{1}{n} \cdot i_s + i_f \tag{2}$$

Applying KVL at node we get:

$$V_{dc} \cdot (2 \cdot V - 1) - i_f \cdot R_f - v_c - L_f \cdot \frac{di_f}{dt} = 0$$

$$\therefore L_f \cdot \frac{di_f}{dt} = \left[v_c + i_f \cdot R_f - V_{dc} \cdot (2 \cdot V - 1) \right] \tag{3}$$

$$v_s - \frac{1}{n} \cdot v_c - v_o - L_s \cdot \frac{di_s}{dt} = 0$$

$$\therefore L_s \cdot \frac{di_s}{dt} = v_s - \frac{1}{n} \cdot v_c - v_o \quad (4)$$

$$i_s = i_F + i_L = \frac{v_o}{Z_F} + i_L$$

$$\therefore v_o = (i_s - i_L) \cdot Z_F \quad (5)$$

$$V = \frac{1}{2} \cdot v_c^*(t) + \frac{1}{2} \quad (6)$$

Let the sate variables are,

$$x_1 = v_c \quad \Rightarrow \quad \dot{x}_1 = \frac{dv_c}{dt} \quad (7)$$

$$x_2 = i_r \quad \Rightarrow \quad \dot{x}_2 = \frac{di_f}{dt} \quad (8)$$

$$x_3 = i_s \quad \Rightarrow \quad \dot{x}_3 = \frac{di_s}{dt} \quad (9)$$

Re-writing the equations (2-4) using equations (7-9):

$$\dot{x}_1 = 0 \cdot x_1 + \frac{1}{C_f} \cdot x_2 + \frac{1}{n \cdot C_f} \cdot x_3 \quad (10)$$

$$\dot{x}_2 = \left(-\frac{1}{L_f}\right) \cdot x_1 + \left(-\frac{R_f}{L_f}\right) \cdot x_2 + 0 \cdot x_3 + \frac{V_{dc}}{L_f} \cdot (2 \cdot V - 1) \quad (11)$$

$$\dot{x}_3 = \frac{1}{n \cdot L_s} \cdot x_1 + 0 \cdot x_2 + \left(-\frac{Z_F}{L_s}\right) \cdot x_3 + \left(\frac{v_s}{L_s} + \frac{i_L \cdot Z_F}{L_s}\right) \quad (12)$$

The equivalent state-space model can be presented as:

$$\begin{bmatrix} \dot{x}_1 \\ \dot{x}_2 \\ \dot{x}_3 \end{bmatrix} = \begin{bmatrix} 0 & \frac{1}{C_f} & \frac{1}{n \cdot C_f} \\ -\frac{1}{L_f} & -\frac{R_f}{L_f} & 0 \\ \frac{1}{n \cdot L_s} & 0 & \frac{Z_F}{L_s} \end{bmatrix} \begin{bmatrix} x_1 \\ x_2 \\ x_3 \end{bmatrix} + \begin{bmatrix} 0 & 0 & 0 \\ \frac{1}{L_f} & 0 & 0 \\ 0 & \frac{1}{L_f} & \frac{Z_F}{L_s} \end{bmatrix} \begin{bmatrix} V_{dc} \\ v_s \\ i_L \end{bmatrix} \quad (13)$$

$$y = x_1 = v_c = \begin{bmatrix} 1 & 0 & 0 \end{bmatrix} \begin{bmatrix} x_1 \\ x_2 \\ x_3 \end{bmatrix} + \begin{bmatrix} 0 & 0 & 0 \end{bmatrix} \begin{bmatrix} V_{dc} \\ v_s \\ i_L \end{bmatrix} \quad (14)$$

Equation (13) is a state equation and equation (14) is an output equation. Comparing them with the standard form,

$$\dot{\bar{x}} = A\bar{x} + B\bar{u} \quad (15)$$

$$\bar{y} = C \cdot \bar{x} + D \cdot \bar{u} \quad (16)$$

These yields:

$$A = \begin{bmatrix} 0 & \frac{1}{C_f} & \frac{1}{n \cdot C_f} \\ -\frac{1}{L_f} & -\frac{R_f}{L_f} & 0 \\ \frac{1}{n \cdot L_s} & 0 & \frac{Z_F}{L_s} \end{bmatrix} \quad (17)$$

$$B = \begin{bmatrix} 0 & 0 & 0 \\ \frac{1}{L_f} & 0 & 0 \\ 0 & \frac{1}{L_f} & \frac{Z_F}{L_s} \end{bmatrix} \quad (18)$$

$$C = \begin{bmatrix} 1 & 0 & 0 \end{bmatrix} \quad (19)$$

$$D = \begin{bmatrix} 0 & 0 & 0 \end{bmatrix} \quad (20)$$

Now Transfer Function of the system is given by:

$$G(s) = C[sI - A]^{-1} B + D \quad (21)$$

3. Stability Analysis

Fig. 3 shows an equivalent single-phase circuit of the system considering current and voltage harmonics produced by EAF.

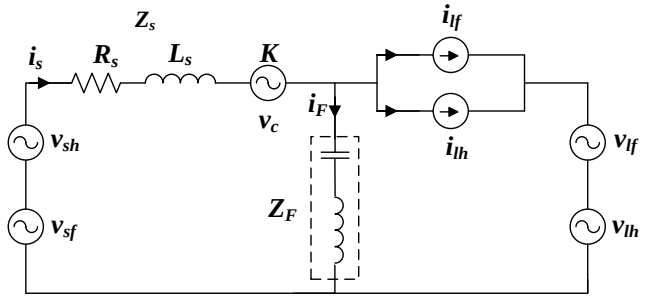

Fig. 3 Single phase equivalent circuit of main system

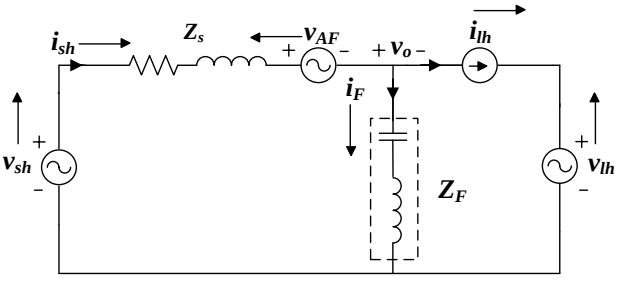

Fig. 4. Single phase equivalent harmonic circuit of main system

Fig. 4 shows single-phase equivalence harmonic circuit of system under consideration. The EAF is represented by harmonic current and harmonic voltage source. From the equivalent circuit shown in Fig. 4, it is obtained:

$$v_o = (i_{sh} - i_{lh}) \cdot Z_F \tag{22}$$

$$v_{AF} = K \cdot i_{sh} \tag{23}$$

Applying KVL:

$$v_{sh} - i_{sh} \cdot Z_S - v_{AF} - v_o - v_{lh} = 0$$

$$\therefore v_{sh} - i_{sh} \cdot Z_S - (K \cdot i_{sh}) - (i_{sh} - i_{lh}) \cdot Z_{F_O} - v_{lh} = 0$$

$$\therefore v_{sh} - i_{sh} \cdot Z_S - K \cdot i_{sh} - i_{sh} \cdot Z_F + i_{lh} \cdot Z_F - v_{lh} = 0$$

$$\therefore (v_{sh} - v_{lh}) - i_{sh}(Z_S + K + Z_F) + i_{lh} \cdot Z_F = 0$$

$$\therefore i_{sh} = \frac{(v_{sh} - v_{lh})}{(Z_S + K + Z_F)} + \frac{Z_F}{(Z_S + K + Z_F)} \cdot i_{lh} \tag{24}$$

With respect to the performance of the compensation, the system behaves like a closed-loop control system. Equation (24) can be represented by traditional closed-loop model of composite filter as shown in Fig. 5. Therefore, the analysis in the‘s’ domain could be developed with the help of block diagram shown in Fig. 6.

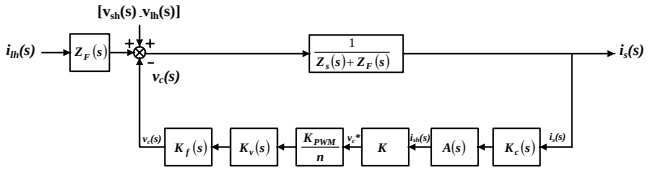

Fig. 5 Block diagram of closed loop model of CF

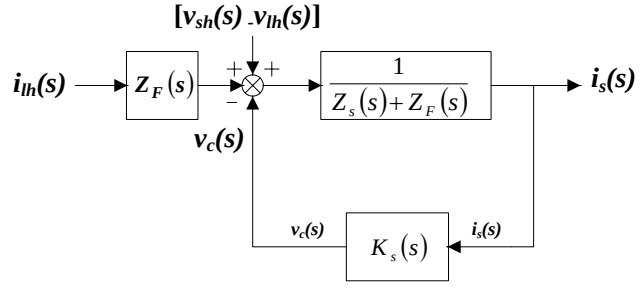

Fig. 6 Reduced block diagram of closed loop model of CF

The open-loop transfer function $k(s)$ from input source current to output voltage can be obtained as:

$$k(s) = \frac{v_c(s)}{I_S(s)} = k_c(s) \cdot A(s) \cdot \frac{K_{PWM}}{n} \cdot k_v(s) \cdot k_f(s) \tag{25}$$

where, $k_c(s) = \frac{k_c}{T_c \cdot s + 1}$, $A(s) = \frac{s^2 + \omega^2}{s^2 + m \cdot s + \omega^2}$, $k_v(s) = \frac{k_v}{T_v \cdot s + 1}$, (Generally, $T_v = \frac{1}{5}$ of carrier wave period (neglecting the sidebands of the switching frequency and the dead time), $k_f(s) = \frac{R_f \cdot C_f \cdot s}{L_f \cdot C_f \cdot s^2 + R_f \cdot C_f \cdot s + 1}$, it can be alternatively expressed as= $\frac{1}{T^2 \cdot s^2 + 2 \cdot \xi \cdot T \cdot s + 1}$, where $T = \sqrt{L_f \cdot C_f}$ (that controls the shape of the transfer function in the vicinity of the $f_0 = \frac{1}{2 \cdot \pi \cdot T}$ respectively.

$$L_f = \frac{n \cdot k}{2 \cdot \pi \cdot f_v} \tag{26}$$

where, $k = \left(\frac{3 \cdot V^2}{S} \right)$,

$$f_{cf} = \frac{1}{2 \cdot \pi \cdot \sqrt{L_f \cdot C_f}} \Rightarrow C_f = \frac{1}{(2 \cdot \pi)^2 \cdot L_f \cdot (f_{cf})^2} \tag{27}$$

$$\xi = \frac{R_f}{2} \cdot \sqrt{\frac{C_f}{L_f}} \Rightarrow R_f = 2 \cdot \xi \cdot \sqrt{\frac{L_f}{C_f}} \tag{28}$$

Where, ξ =damping factor.

$$\therefore 1.6\sqrt{\frac{L_f}{C_f}} \le R_f \le 0.8\sqrt{\frac{L_f}{C_f}} \tag{29}$$

4. Calculations

A three-phase 550/50 Hz, 100 MVA power rating an electric arc furnace is considered as a non-linear load. The detailed specifications are as follows:

Table 1 EAF Distribution Network Parameters

Parameter	Value	Parameter	Value
V	550 V	S	1 MVA
f	50 Hz	C_{dc}	200 µF
S	10 MVA	V_{dc}	400 V
R_s	0.1 Ω	f_v	25 kHz
L_s	110 µs	n	25
R_c	100 µs	ξ	0.6
L_c	0.23 mH	k_c	0.2
τ_c	100 µs	m	100
k_v	40	K_{PWM}	200/16
τ_v	8 µs		

Neglecting Kelvin effect, eddy current effect and attenuation of filter's gain, the maximum gain will be calculated using (26) to (29) [10]:

$$k = \left(\frac{3 \cdot V^2}{S}\right) = 3 \cdot \left(\frac{\left(550/\sqrt{3}\right)^2}{10^7}\right) = 0.0303$$

$$k_c(s) = \frac{k_c}{\tau_c \cdot s + 1} = \frac{0.2}{100 \times 10^{-6} \cdot s + 1} = \frac{0.2}{1 \times 10^{-4} \cdot s + 1}$$

$$A(s) = \frac{s^2 + \omega^2}{s^2 + m \cdot s + \omega^2} = \frac{s^2 + (2 \cdot \pi \cdot 50)^2}{s^2 + 100 \cdot s + (2 \cdot \pi \cdot 50)^2}$$

$$\therefore A(s) = \frac{s^2 + 314^2}{s^2 + 100 \cdot s + 314^2}$$

$$k_v(s) = \frac{k_v}{T_v \cdot s + 1} = \frac{40}{8 \times 10^{-6} \cdot s + 1}$$

$$L_f = \frac{n \cdot k}{2 \cdot \pi \cdot f_v} = \frac{25 \times 0.03025}{2 \cdot \pi \cdot 25 \times 10^3} = 4.8144 \times 10^{-6}\ H$$

$$C_f = \frac{1}{(2 \cdot \pi)^2 \cdot L_f \cdot (f_{cf})^2} = \frac{1}{(2 \cdot \pi)^2 \cdot (4.816 \times 10^{-6}) \cdot \left(\frac{25 \times 10^3}{10}\right)^2}$$

$$\therefore C_f = 8.4181 \times 10^{-4}\ F$$

$$R_f = 2 \cdot \xi \cdot \sqrt{\frac{L_f}{C_f}} = 2 \cdot (0.6) \cdot \sqrt{\frac{4.816 \times 10^{-6}}{8.424 \times 10^{-4}}} = 0.0908\ \Omega$$

$$k_f(s) = \frac{R_f \cdot C_f \cdot s}{L_f \cdot C_f \cdot s^2 + R_f \cdot C_f \cdot s + 1}$$

$$= \frac{(0.09073) \cdot (8.424 \times 10^{-4}) \cdot s}{(4.816 \times 10^{-6}) \cdot (8.424 \times 10^{-4}) \cdot s^2 + (0.09073) \cdot (8.424 \times 10^{-4}) \cdot s + 1}$$

$$= \frac{(7.639 \times 10^{-5}) \cdot s}{(4.053 \times 10^{-9}) \cdot s^2 + (7.639 \times 10^{-5}) \cdot s + 1}$$

Finally the feedback path transfer function given by (25):

$$k_s(s) = \frac{0.2}{1 \times 10^{-4} \cdot s + 1} \cdot \frac{s^2 + 314^2}{s^2 + 100 \cdot s + 314^2} \cdot \frac{200}{16} \cdot \frac{40}{8 \times 10^{-6} \cdot s + 1} \cdot \frac{(7.639 \times 10^{-5}) \cdot s}{(4.053 \times 10^{-9}) \cdot s^2 + (7.639 \times 10^{-5}) \cdot s + 1} \quad (30)$$

As per [24], the time constant of leading compensator can be calculated as:

$$K_P = \frac{(4.053 \times 10^{-9})}{(7.639 \times 10^{-5})} = 0.530 \times 10^{-4}$$

Transfer function of phase-lead compensator can be given by:

$$K_P(s) = 0.530 \times 10^{-4} \cdot s + 1 \quad (31)$$

Now the transfer function of feedback path with phase-lead compensator can be given by:

$$K'_s(s) = (0.530 \times 10^{-4} \cdot s + 1) \cdot K_s(s) \quad (32)$$

5. Simulation Results

Simulation results of Bode plot for functions $K_s(s)$ and $K'_s(s)$ are obtained by (30) and (32) respectively. Obtained simulation results are shown in Fig. 7 and Fig. 8 respectively.

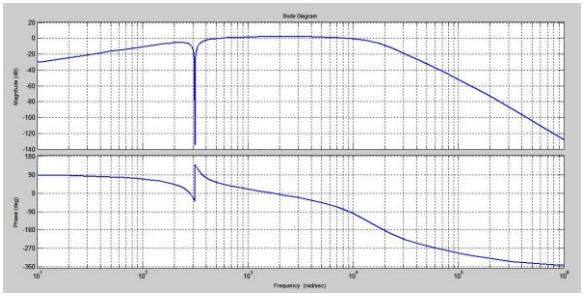

Fig. 7. Magnitude and Phase Bode Plot for function k(s)

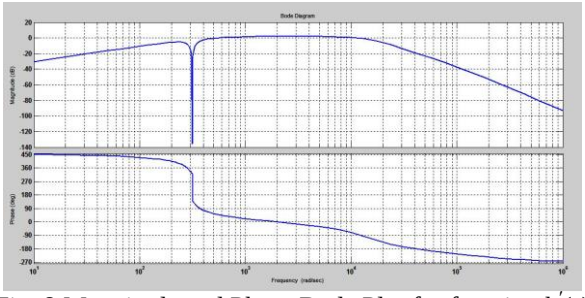

Fig. 8 Magnitude and Phase Bode Plot for function k'(s)

Comparison of simulated results shown in Fig. 8 with Fig. 7 shows that the gain margin and the phase margin of the open loop transfer function can be improved a lot. Also, the cut-off frequency boosted when, the lead compensation is adopted. Quantified results of gain margin and phase margin are tabulated in Table 2.

Table 2 Bode plot output

Parameter	Gain margin	Phase margin
$K_s(s)$	0.506 dB	1.45 deg
$K'_s(s)$	50.1 dB	40.9 deg

It can be seen that the gain margin and the phase margin has increased considerably by lead compensation strategy.

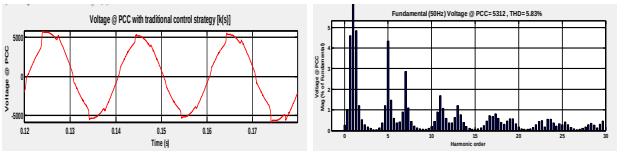

(a) (b)

Fig. 9 (a) Voltage @ PCC (b) harmonic spectrum (with tradition control strategy k(s))

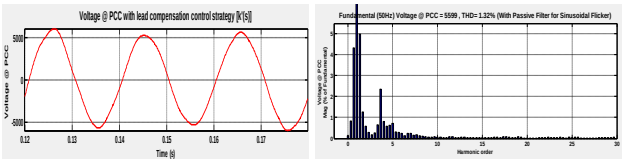

(a) (b)

Fig. 10 (a) Voltage @ PCC (b) harmonic spectrum (with lead compensation control strategy $k^{'}(s)$)

Table 3 THD improvement

Parameter	THD	% THD improvement
$K_S(s)$	5.83	77.35
$K_S^{'}(s)$	1.32	

Comparison of Fig. 9 and Fig. 10 shows improved voltage wave at PCC as well as total harmonic distortion (THD) after lead compensation application. Quantified results are tabulated in Table 3. THD has improved by 77.35% after lead compensation application. Maximum gain is calculated by neglecting Kelvin effect, eddy current effect and attenuation of filter's gain, which could be a limitation of this analysis.

6. Conclusion

In this paper, a state-space averaging model has been constructed to analyze the stability of CF used for PQ improvement of EAF distribution network. It is difficult to obtain a better filter performance confined to the system stability by the traditional control strategy, taking into account the time delay in the control circuit. The analysis has indicated that the time delay can cause a stability problem. Therefore, a phase-lead compensation strategy has been proposed to eliminate the effect of time delay. It suggests method of lead compensation for $K_s(s)$ to increase the value of the cut-off frequency. The increase of gain margin and phase margin can clearly clarify that the proposed control strategy improves the system stability compared with the traditional control strategy. Simulation verifies the validity of the developed theory. This work does not include experimental analysis. The real time implementation of the proposed work can be given a purview as future work. One can analyze the stability considering advanced stability analysis methods to get rid of shortcoming of traditional control strategy presented in this paper-as future work.

7. Nomenclature

n =transformation ratio

v_c =controlled inverter output voltage

V_{dc} =dc bus voltage

i_s =source current

i_L =load current

L_f =carrier filter inductance

R_f =carrier filter resistance

L_f =carrier filter inductance

C_f =carrier filter capacitance

i_f =inductor current through L_f

v_s =source voltage

v_c =voltage in the secondary of the coupling transformer

$v_c^*(t)$=input reference voltage

v_o =output voltage seen by the load

v_{sf} = fundamental components of source voltage

v_{sh} =harmonics components of source voltage

v_{lf} =fundamental components of load voltage

v_{lf} =harmonics components of load voltage

i_{lf} = fundamental components of current injected by load

i_{lh} =harmonics components of current injected by load

Z_S =source impedance

Z_F =passive filter impedance

$k_c(s)$=Transfer function of the sensor modulating circuit

k_c =gain of the sensor modulating circuit

T_c =time constant of the sensor modulating circuit

$A(s)$=Transfer function of the harmonics calculating circuit

m =internal gain of the harmonics calculating circuit

K_{PWM} =Inverter gain of the harmonics calculating circuit

$k_v(s)$=transfer function of the inverter

k_v =gain determined by the speed of the processor/related software

T_v =time constant determined by the speed of the processor/related software

$k_f(s)$= Transfer function of the output carrier filter circuit

ξ =damping factor (chosen between 0.4 to 0.6)

S =apparent output of the load

V =phase voltage

f_{cf} =cross-over frequency of the filter

f_v =carrier frequency

References

[1] Douglas Andrews, Martin T. Bishop and John F. Witte, *Harmonic Measurements, Analysis, and Power Factor Correction in a Modern Steel Manufacturing Facility*, IEEE TRANSACTIONS ON INDUSTRY APPLICATIONS, VOL. 32, NO. 3, MAY-JUNE 1996, pp. 617-624.

[2] Janusz Mindykowski, Tomasz Tarasiuk and Piotr Rupnik, *Problems Of Passive Filters Application In System With Varying Frequency* , 9th International Conference, Electrical Power Quality and Utilization, 9-11 October 2007, Barcelona.

[3] Juan W. Dixon, Gustavo Venegas and Luis A. Mor´an, *A Series Active Power Filter Based on a Sinusoidal Current-Controlled Voltage-Source Inverter*, IEEE TRANSACTIONS ON INDUSTRIAL ELECTRONICS, VOL. 44, NO. 5, OCTOBER 1997 pp. 612-620.

[4] G. Carpinelli, Member and A. Russo, *Comparison of some Active Devices for the Compensation of DC Arc Furnaces*, IEEE Bologna Power Tech Conference, June 23-26, Bologna, Italy.

[5] P. Salmerón and S. P. Litrán, *Improvement of the Electric Power Quality Using Series Active and Shunt Passive Filters*, IEEE TRANSACTIONS ON POWER DELIVERY, VOL. 25, NO. 2, APRIL 2010, pp. 1058-1067.

[6] F. Z. Peng, H. Akagi and A. Nabae, *A New approach to Harmonic Compensation in Power System-a combined system of shunt passive and series active filters*, IEEE Transactions on Industrial Applications, Vol. 26, Issue 1, pp. 983-990, Nov/Dec'90.

[7] F. Z. Peng, H. Akagi and A. Nabae, *Compensation characteristics of the combined system of Shunt Passive and Series active Filters*, IEEE Transactions on Industrial Applications, Vol. 29, Issue 6, pp. 144-152, Jan/Feb'93.

[8] L. Xu, E. Acha and V. G. Agelidis, *A New Synchronous Frame-base control strategy for a Series Voltage and Harmonic Compensator*, Proceedings of Applied Power Electronics Conf., 2001 IEEE. Vol. 2. pp. 1274-1280, 2001.

[9] S. rianthumrong, H. Fujita and H. Akagi, *Stability Analysis of a Series Active Filter integrated with a double-series diode rectifier*, IEEE 31st Annual Power Electronics Specialists Conf., Vol. 3, pp. 1305-1311, 2000.

[10] Hadi Y. Kanaan and Kamal Al-Haddad, *Design of a New Multiple-Loops Linear Controller for a Three-Phase Series Active Voltage Harmonic Compensator*, IEEE ICIT, Maribor, Slovenia, 2003, pp. 575-580.

[11] Salem Rahmani, Kamal Al-Haddad and Hadi Y. Kanaan, *Average Modelingand Hybrid Control of a Three-Phase Series Hybrid Power Filter*, IEEE ISIE July 9-12, 2006, Montreal, Quebec, Canada, pp. 919-924.

[12] Liqing Tong, Zhaoming Qian, Yantao Song, Naixing Kuang and Fang Z. Peng, *Analysis and Design of a Novel Phase-lead Compensation Control Strategy for the SHAPF*, IEEE APC 2007, pp. 692-697.

[13] Cunlu Dang, Defu Wang, Xiaoying Zhang and Lingli Gan, *Study of a New Hybrid Active Power Filter*, Pacific-Asia Conference on Circuits, Communications and Systems, IEEE Computer Society, pp-224-227.

[14] WeiMinWu, LiQuing Tong, MingYue Li, Z. M. Quian, Zheng Yu Lu and F. Z Peng, *A New Control Strategy for Series Type Active Power Filter*, IEEE 35st Annual Power Electronics Specialists Conf., Aachen, Germany, pp. 3054-3059, 2004